Proceedings of the 21st ICSMGE, Vienna, Austria, 14 – 19 June 2026. Pistrol, Adam & Schweiger (eds.)
Published by: ÖGG, Austrian Society for Geomechanics, Salzburg, Austria, ISBN 978-3-9503898-4-5
https://doi.org/10.53243/ICSMGE2026-1833

How can Controlled Modulus Columns (CMC) mitigate liquefaction

Fanny Maucotel, Jérôme Racinais, Cyril Plomteux
Design Support Office, Menard, France, fanny.maucotel@menard-mail.com

ABSTRACT: Ground improvement solutions are widely used to mitigate liquefaction risks. For relatively clean sandy soils, Vibrocompaction and Dynamic Compaction are well-suited, while Stone Columns or Soil Mixing are typically employed for soils with higher fines content. In the case of heavily loaded structures, these ground improvement techniques are often combined with classic deep foundations to support the load. An alternative to these traditional solutions under seismic conditions including liquefaction, is the use of Controlled Modulus Columns (CMC), a type of rigid inclusions. CMCs offer practical and economic advantages, effectively solving settlement, bearing capacity (in both static and seismic conditions), and liquefaction issues. CMCs should be installed using soil-displacement augers to achieve key benefits for liquefaction mitigation, such as soil densification, an increase in the at-rest earth pressure coefficient, and to a lesser extent, in shear stress acting on the soil. While in some instances CMCs can fully mitigate liquefaction, in others they only partially do so. Particularly in the latter case, their integrity must be verified in terms of geotechnical capacity and structural resistance. This paper introduces an advanced analytical method using various simplified approaches for the seismic design of CMCs, addressing liquefaction. This methodology has been validated through site feedback, with an example provided to illustrate its application.

KEYWORDS: Rigid inclusions, seismic design, liquefaction mitigation, geotechnical and structural verifications.

1 INTRODUCTION

Soil liquefaction is a seismic phenomenon in which saturated, loose granular soils lose strength and stiffness due to elevated pore water pressure, resulting in ground deformation and potential structural failure. This process poses a critical hazard to infrastructure in regions with high seismicity and soft soil conditions. Over the past decades, a range of ground improvement techniques has been developed to mitigate liquefaction risk, with selection typically based on soil type and project requirements.

For relatively clean sandy soils, vibrocompaction and dynamic compaction are widely used to increase density and reduce liquefaction susceptibility. Soils with higher fines content, such as silts and clays, require alternative techniques, including stone columns to improve drainage and shear strength, and jet grouting or soil mixing to increase overall strength. These methods often need to be supplemented with deep foundations to support heavily loaded structures, particularly where seismic resilience is a key design objective.

Controlled Modulus Columns (CMCs) have recently emerged as a versatile ground improvement solution for seismic applications. Installed using displacement augers, CMCs provide rigid inclusions without generating vibration, making them suitable for urban environments and vibration-sensitive facilities. They simultaneously address multiple geotechnical challenges, including bearing capacity enhancement, settlement control, and liquefaction mitigation.

Liquefaction mitigation by CMCs operates through three primary mechanisms: (i) densification of the surrounding soil during installation, (ii) an increase in the horizontal earth pressure coefficient (K_0) due to lateral soil displacement, and (iii) a reduction in vertical stress, with a smaller contribution from reduced shear stress. These mechanisms are most effective when CMCs are anchored in a non-liquefiable stratum, ensuring continuous load transfer and structural integrity even if liquefaction occurs in overlying layers. Inadequate anchorage may compromise system performance or cause structural damage under seismic loading.

Although complete liquefaction mitigation can be achieved in certain conditions, partial mitigation is more common, particularly in complex stratigraphic profiles, where transitional layers may still exhibit safety factors against liquefaction below unity. In such cases, verification of CMC integrity is essential, encompassing both geotechnical performance and structural resistance to seismic effects.

This paper presents an analytical framework for the CMCs design for liquefaction mitigation. The framework integrates simplified yet robust procedures for assessing liquefaction potential and settlement. Its applicability is demonstrated through a detailed case study.

2 MECHANISMS OF LIQUEFACTION MITIGATION BY CMCs

CMCs, when installed using full-displacement augers, mitigate liquefaction through three interrelated mechanisms that improve soil behavior under seismic loading. These mechanisms, discussed in detail in the following subsections, include:

- densification of the surrounding soil,
- an increase in the horizontal earth pressure coefficient (K_0),
- and a reduction in shear stress.

Collectively, these effects contribute to a significant enhancement of the soil's resistance to liquefaction and its overall seismic performance.

2.1 *Soil densification*

The installation of CMCs using full-displacement augers induces lateral displacement of the surrounding soil, resulting in densification. This process increases the relative density (D_r) of the soil, thereby improving its resistance to liquefaction. The degree of densification depends on several factors:

- Soil compactability, typically assessed through Cone Penetration Tests (CPT) using the Massarsch diagram (1991), as shown in Figure 1. Originally developed from vibrocompaction case histories, this diagram provides a conservative estimate of soil response to lateral displacement. While the range of soils compactible by displacement methods (e.g., compaction grouting) is generally broader under drained conditions, the Massarsch diagram remains a reliable tool for preliminary assessment. Clean sands generally exhibit a higher potential for densification compared to silty or clayey soils.
- Replacement ratio (τ), defined as the ratio of the column cross-sectional area to the treated ground area. Higher values of τ generally result in greater densification, as more

material is introduced into the soil matrix, increasing confinement and reducing void ratios.

- Execution speed, which influences the degree of soil displacement and, consequently, the amount of densification achieved. Faster installation may reduce the time available for pore pressure dissipation, particularly in low-permeability soils. Although installation speed does not directly govern drainage conditions, it interacts with the soil's permeability, which determines whether the soil response during installation is drained or undrained. Effective densification occurs primarily under drained conditions, where pore pressures can dissipate and soil particles can rearrange and compact. To achieve this, installation speed must be carefully controlled in relation to the soil's hydraulic properties.

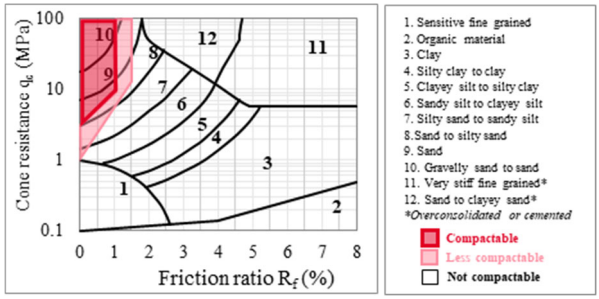

Figure 1. Soil compactability from Massarsch (1991) diagram, based on soil classification chart by Roberston et al. (1986).

Densification resulting from CMC installation can be assessed through two approaches.

The first is based on the improvement factor (I), which relates the cone resistance of the improved soil ($q_{c,I}$) to that of the unimproved soil ($q_{c,U}$) using the expression:

$$q_{c,I} = I \cdot q_{c,U} \tag{1}$$

The improvement factor can be derived from empirical correlations such as Ménard's Standard D60, Siegel et al. (2007), or calibrated using site-specific data in a user-defined approach.

The second method involves estimating the increase in relative density (ΔD_r) from the replacement ratio (τ). This is commonly done using empirical correlations that relate CPT resistance to relative density, such as those proposed by Robertson (1986), Jamiolkowski (2001), and Baldi et al. (1986).

To ensure realistic estimates, the densification ratio must be corrected for the heave effect—the upward displacement of soil during column installation. A correction factor α, typically set at 50% in preliminary design, is recommended as a conservative estimate. This adjustment accounts for the partial loss of densification due to volume expansion and ensures that the calculated improvement remains within safe design margins.

Beyond liquefaction mitigation, densification also contributes to settlement control and increased bearing capacity.

2.2 *Increase in lateral earth pressure coefficient*

The installation of CMCs using full-displacement augers causes lateral displacement of the surrounding soil, leading to an increase in the horizontal earth pressure coefficient at rest (K_0). This enhanced confinement improves the soil's resistance to liquefaction. The mechanism is driven by the principles of cavity expansion, whereby the lateral displacement of soil generates additional horizontal stress in the adjacent soil mass.

Typically, the post-installation horizontal stress exceeds the initial condition, with $K_{0,I} / K_{0,U} > 1$ observed in most cases. Here, $K_{0,I}$ denotes to the horizontal earth pressure coefficient of the improved soil after CMC installation, and $K_{0,U}$ at rest in the unimproved soil. Predicting $K_{0,I}$ is challenging due to its dependence on soil type, stiffness, and installation parameters. Numerical simulations, such as those based on the Finite Element Method (FEM), are commonly employed for estimation.

Empirical approaches also provide useful benchmarks for design, especially when site-specific modeling is unavailable. For example, Domingues et al. (2007) adopted $K_{0,I} = 0.7$, while Priebe (1995) assumed $K_{0,I} = 1.0$.

The increase in lateral earth pressure coefficient must be considered in liquefaction analyses, as it directly affects the cyclic resistance ratio (CRR) and the safety factor against liquefaction initiation (FS). Experimental work by Ishihara et al. (1977, 1985), after Salgado, Boulanger, Mitchell (1997), and Idriss & Boulanger (2008), demonstrated the influence of horizontal earth pressure coefficient on liquefaction resistance through cyclic torsional shear tests. Their findings showed that the CRR of anisotropically consolidated soils ($K_0 \neq 1$) can be approximated from the CRR of isotropically consolidated soils ($K_0 = 1$) using the following relationship:

$$CRR_{K_0 \neq 1} = \frac{(1 + 2K_0)}{3} CRR_{K_0 = 1} \tag{2}$$

In the context of CMCs, where the coefficient increases from $K_{0,U}$ to $K_{0,I}$, the relative improvement in CRR can be estimated using a simplified ratio (Cristovao et al. 2015):

$$\Delta CRR_{K_{0,I};K_{0,U}} = \frac{(1 + 2K_{0,I})}{(1 + 2K_{0,U})} \tag{3}$$

This formulation provides a practical tool for quantifying the gain in liquefaction resistance resulting from the increase in horizontal confinement induced by CMC installation. Accordingly, the cyclic resistance ratio of the improved soil (CRR_I) can be expressed as:

$$CRR_I = CRR_U \times \Delta CRR_{K_{0,I};K_{0,U}} \tag{4}$$

Where CCRu is the cyclic resistance ratio of the unimproved soil.

2.3 *Reduction in shear stress*

CMCs contribute to liquefaction mitigation by reducing the shear stress acting on the surrounding soil, particularly under seismic loading conditions. This effect is quantified using the shear stress reduction coefficient (R_{rd}), which relates the cyclic shear stress ratio of the improved soil CSR_I to that of the unimproved soil CSR_U. The coefficient R_{rd} incorporates both the shear modulus ratio (G_r) and the replacement ratio (τ):

$$CSR_I = CSR_U \times R_{rd} \tag{5}$$

Unlike flexible inclusions such as stone columns, stiff column-type inclusions like CMCs do not accommodate pure shear strain compatibility with the surrounding soil. Consequently, traditional approaches, such as those proposed by Baez & Martin (1993), are considered unconservative when applied to rigid inclusions.

To better account for shear strain incompatibility between CMC and the surrounding liquefied soil, as well as the flexural behavior of the columns, more advanced models have been proposed, notably by Hashin (1983) and Rayamajhi et al. (2014). These models show that when the shear modulus ratio (G_r) is large, the inverse of the reduction coefficient $1/R_{rd}$ tends

toward 1+ 2 τ in the mathematical model by Hashin (1983) and 1 in the simplified numerical model by Rayamajhi et al. (2014).

3 INDICATORS OF LIQUEFACTION VULNERABILITY

While the factor of safety (FS) against liquefaction is widely used to assess triggering conditions, it does not fully capture the potential for surface damage or structural impact. To address this, several complementary indicators have been developed to evaluate the likelihood and severity of liquefaction-induced manifestations. These indicators provide a more comprehensive understanding of site-specific vulnerability and support the design of effective mitigation strategies.

3.1 *Cumulative thickness of liquefiable layers*

The Cumulative Thickness of Liquefiable layers (CTL) is a straightforward yet effective parameter used to estimate the vertical extent of potentially liquefiable soil relative to the total depth of the soil profile, *H*. It is defined as:

$$CTL = \int_0^H (FS < 1)dz \tag{6}$$

CTL serves as a preliminary check for assessing liquefaction vulnerability across a soil profile.

3.2 *Volumetric reconsolidation settlement*

The one-dimensional volumetric reconsolidation settlement (S_{V1D}) estimates the post-liquefaction settlement due to volumetric strain (ε_v), excluding contributions from sand ejecta and shear-induced deformation:

$$S_{1VD} = \int_0^H \varepsilon_v dz \tag{7}$$

ε_v is typically derived from CPT resistance, using empirical correlations such as those proposed by Zhang et al. (2002).

3.3 *Liquefaction potential index*

The Liquefaction Potential Index (LPI), introduced by Iwasaki et al. (1981), quantifies the severity of liquefaction across a soil profile:

$$LPI = \int_0^{20m} F_1 W(z)dz \tag{8}$$

Where W(z) = 10 – 0.5z, F_1 = 1 - FS for FS < 1, F_1 = 0 for FS > 1, and z is the depth below the ground surface.

Interpretation of LPI values is summarized in Table 1.

Table 1. Liquefaction risk classification and associated requirements for soil investigations and countermeasures based on LPI values.

LPI	Liquefaction potential	Detail investigations on soil liquefaction	Countermeasures
0	Very low	Not needed in general	
0-5	Low	Needed only for especially important structures.	Not needed in general
5-15	Rather high	Needed for important structures	Needed in general
> 15	very high	Needed	

3.4 *Ishihara-inspired liquefaction potential index-*

Maurer et al. (2015) proposed a modified version of LPI, known as LPI_{ISH}, which better accounts for the presence of a non-liquefiable crust of thickness H_1, based on Ishihara (1985) boundary curves:

$$LPI_{ISH} = \int_{H_1}^{20m} F_1 \frac{25.56}{z} dz \tag{9}$$

Where F_1 = 1 - FS for FS ≤ 1 and $H_1 \cdot m \leq 3$, F_1 = 0 otherwise, and m = exp[5 / (25.56 (1 - FS))] - 1 for FS ≤ 0.95, m = 100 for FS > 0.95 (Green et al., 2018).

3.5 *Liquefaction severity number*

The Liquefaction Severity Number (LSN), developed by Van Ballegooy et al. (2012), correlates well with observed damage in Christchurch, New Zealand. It is defined as:

$$LSN = 1000 \int_0^H \frac{\varepsilon_v}{z} dz \tag{10}$$

Interpretation of LSN values is provided in Table 2.

Table 2. Liquefaction land effects using LSN.

LSN	Signs of liquefaction	Manifestation severity
0-10	Little to no	Minor effects
10-20	Minor.	Some sand boils
20-30	Moderate	Sand boils and some structural damage
30-40	Moderate to severe	Settlement can cause structural damage.
40-50	Major consequences	Heave and collapse at the ground surface, lateral spreading, introducing differential settlement of structures, and failure of pipelines and other lines.
> 50	Severe damage	Extensive evidence of liquefaction at surface, very high total and differential settlement affecting structures, damage to services with loss of resilience of the populations.

3.6 *Ishihara boundary curves*

The Ishihara boundary curves (1985) offer a simplified method to assess the likelihood of surface damage based on the relative thicknesses of liquefiable (H_2) and surface non-liquefiable (H_1) layers. These curves are particularly useful when CTL is used as an approximation for H_2, although they may oversimplify complex stratigraphic profiles.

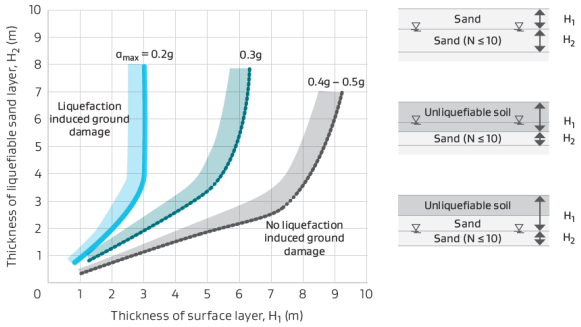

Figure 2. Boundary curves proposed for site identification of liquefaction-induced damage (Ishihara, 1985).

3.7 *Towhata probability chart*

Towhata et al. (2015) developed a probability chart that combines LPI and H_1 to estimate the likelihood of surficial liquefaction manifestation. The chart categorizes risk into zones as shown in Figure 3 and Table 3.

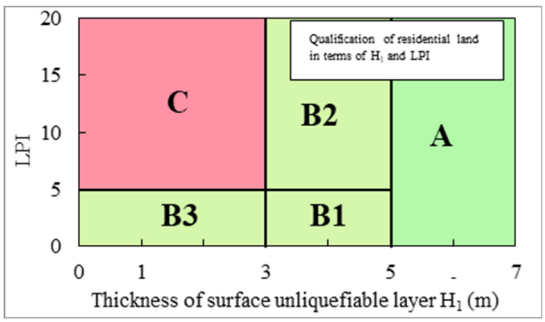

Figure 3. Chart for predicting the probability of severe surficial liquefaction manifestations (Towhata et al. 2016).

Table 3. Probability of severe liquefaction manifestations for zones in the Towhata et al. (2016) chart.

Qualification	Probability of severe liquefaction damage
A	Unlikely to liquefy
B1, B2, B3	Low probability to liquefy
C	High probability to liquefy

The chart suggests that when H_1 is greater than or equal to 5 meters, the probability of surficial liquefaction manifestation is systematically low, regardless of seismic loading conditions. This observation supports the effectiveness of the 5-meter-thick surface-layer confinement in mitigating liquefaction-induced damage.

4 CASE STUDY

This case study focuses on ground improvement works carried out beneath a large-diameter gas tank with a floating roof (volume: 65,000 m³; diameter: 56 m; height: 20 m), located in Fos-sur-Mer, France. The tank is installed on a 1.3-meter-high fill embankment, which serves as a load distribution platform. The site is geotechnically homogeneous both laterally and vertically, with the soil profile summarized in Table 4. The groundwater table is located near the ground surface, increasing the susceptibility of the site to liquefaction.

Table 4. Soil profile of the case study.

N°	Layer	Depth (m)	Thickness (m)	q_c (MPa)	R_f (%)
1	Man made fill	2.4	2.4	3 to 10	0.5
2	Silty clay	4.7	2.3	0.3 to 0.5	1 to 2
3	Silty sand	6.2	1.5	5 to 6	0.35
4	Sandy clay	6.2	0.4	0.8 to 3	3
5	Clayey sand	6.8	0.2	6	0.7
6	Gravel	> 8.8	> 2	> 15	0.2

Where q_c is the CPT cone resistance and R_f is the friction ratio.

The site is situated in a moderate seismic zone, as defined by national seismic zoning regulations. The design earthquake is characterized by a moment magnitude (M_w) of 6.5 and a peak ground acceleration (PGA) of 0.25g.

To address these conditions, the ground was reinforced using CMCs installed with full-displacement augers. The columns were arranged on a 1.4 m × 1.4 m square grid, with a diameter of 360 mm, corresponding to a replacement ratio of 5.2%. This relatively dense grid was selected to mitigate liquefaction risk and ensure both static and post-seismic foundation performance, with particular emphasis on controlling total and differential settlements, very sensitive for floating roof tanks.

To evaluate the effectiveness of the ground improvement works, CPTs, commonly used to assess densification and liquefaction potential, were performed both before and after the installation of CMCs. The results for two different locations are presented in Figure 4.

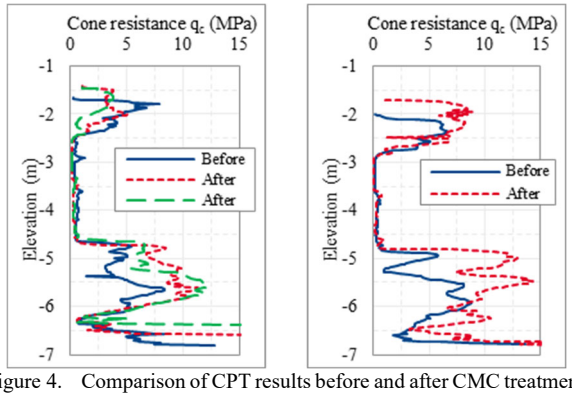

Figure 4. Comparison of CPT results before and after CMC treatment.

The ground improvement strategy specifically targeted the liquefiable sand layers, aiming to achieve measurable densification through displacement-induced compaction. At shallow depths, the impact of CMC installation on q_c was limited. Although the surface soils were likely compactable, the lack of confinement near the ground surface resulted primarily in heave and deformation, rather than effective densification. In contrast, significant improvement was observed in the deeper sand layers, where confinement is greater. Post-treatment CPT data show an increase in cone resistance by nearly a factor of two, providing strong justification for the reduced liquefaction potential in these layers.

5 APPLICATION OF THE PREDICTION METHODOLOGY

In the context of the case study, the mechanisms of liquefaction mitigation by CMCs described in section 2 were applied using the available pre-CPT data.

Figure 5 illustrates the soil compactability profile of the site using the Massarsch diagram (1991), based on the CPT data, related soil behaviour index I_c and soil classification chart by Roberston et al. (1986). This analysis identified the sandy layers as more or less compactable, particularly layers 1, 3 and 5.

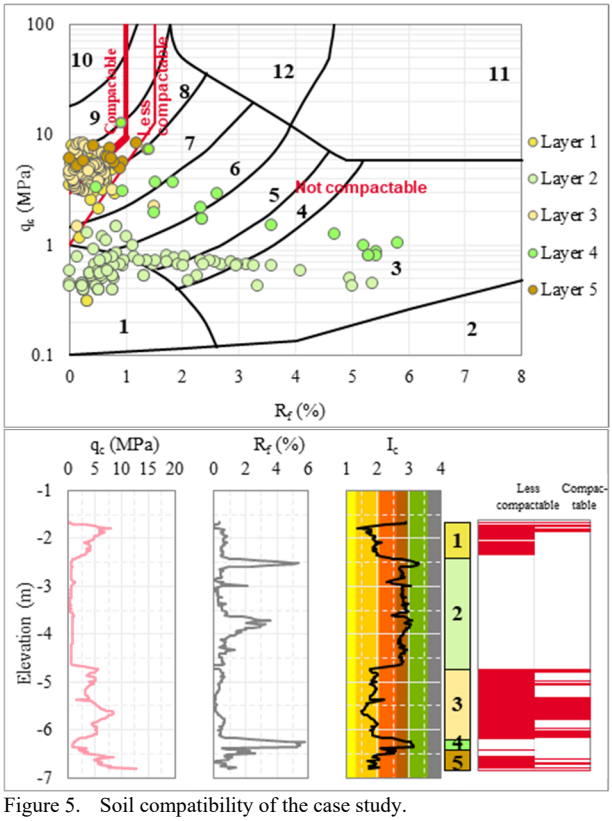

Figure 5. Soil compatibility of the case study.

For the densification effect, the improvement factor due to CMC installation was estimated using the empirical correlations proposed by Siegel et al. (2007). To account for the heave effect during installation, a correction factor α of 50% was applied, in line with conservative design practice.

For the K_0 increase, $K_{0,U}$ was estimated using the Jacky (1944) formula, with the soil friction angle derived from CPT data based on the correlation by Robertson and Campanella (1983). $K_{0,I}$ was assumed to be 0.7, following the empirical findings of Domingues et al. (2007).

For the shear stress reduction, R_{rd} was derived from the analytical model proposed by Hashin (1983), which accounts

for the stiffness contrast between the rigid inclusions and the surrounding soil. In this case, the shear modulus ratio was approximately 300.

Figure 6 illustrates the contribution of each mitigation mechanism to the overall safety factor against liquefaction. The figure also presents a comparison between the predicted value $q_{c,I}$ and the post-CPT measurements. The two datasets are in the same range, with the predicted values generally on the conservative side. At shallow depths, however, the predicted values tend to overestimate improvement due to limited confinement.

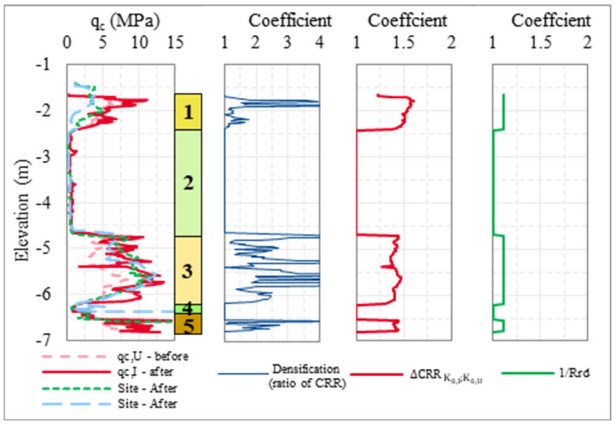

Figure 6. Contribution of the mitigation mechanism.

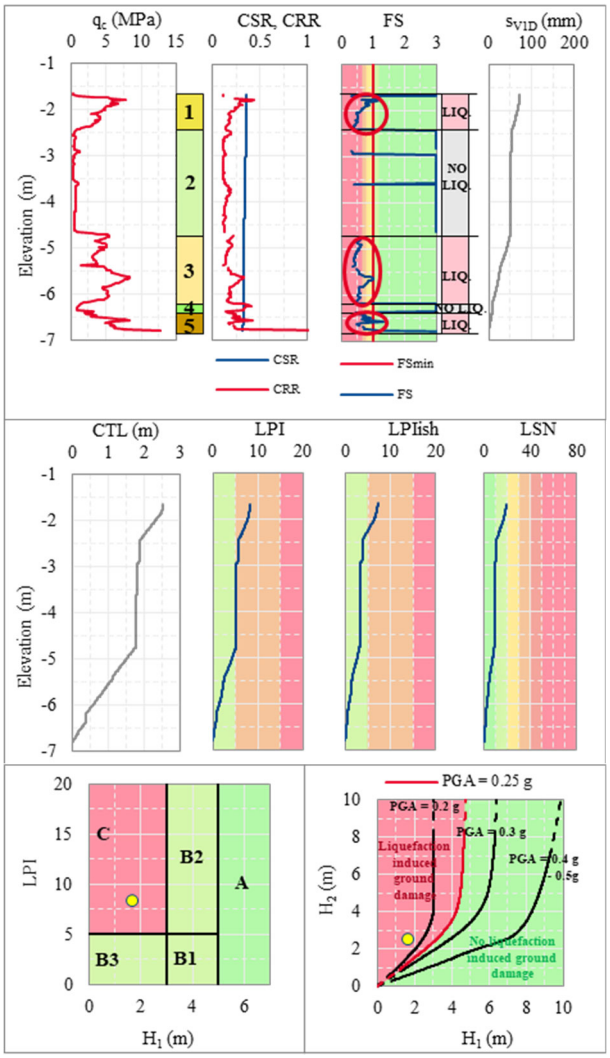

Summary	
S_{V1D} (mm)	73
H_1 (m)	1.7
CTL=H_2 (m)	2.5
LPI	8
LPIish	7
LSN	19
Ishirara (1985)	Damage
Towhata (2015)	C

Figure 7. Liquefaction analysis prior to CMC reinforcement

To assess the initial condition of the ground prior to any treatment, the safety factor against liquefaction was calculated using CPT data and the methodology proposed by Youd et al. (2001), based on the NCEER/NSF guidelines from 1996 and 1998. The results of this analysis are presented in Figure 7.

The analysis identified several liquefiable layers at various depths. Using the approach developed by Zhang et al. (2002), the estimated liquefaction-induced settlement was approximately 73 mm. All relevant liquefaction vulnerability indicators were plotted to qualitatively evaluate whether the predicted liquefaction poses a risk of surface damage or structural impact. While these indicators are based on simplified assumptions, their combined interpretation provides a reliable estimate of the potential consequences for the structure. In this case, under the initial ground conditions, the occurrence of liquefaction is expected to result in significant ground deformation, including large settlements and potential structural damage.

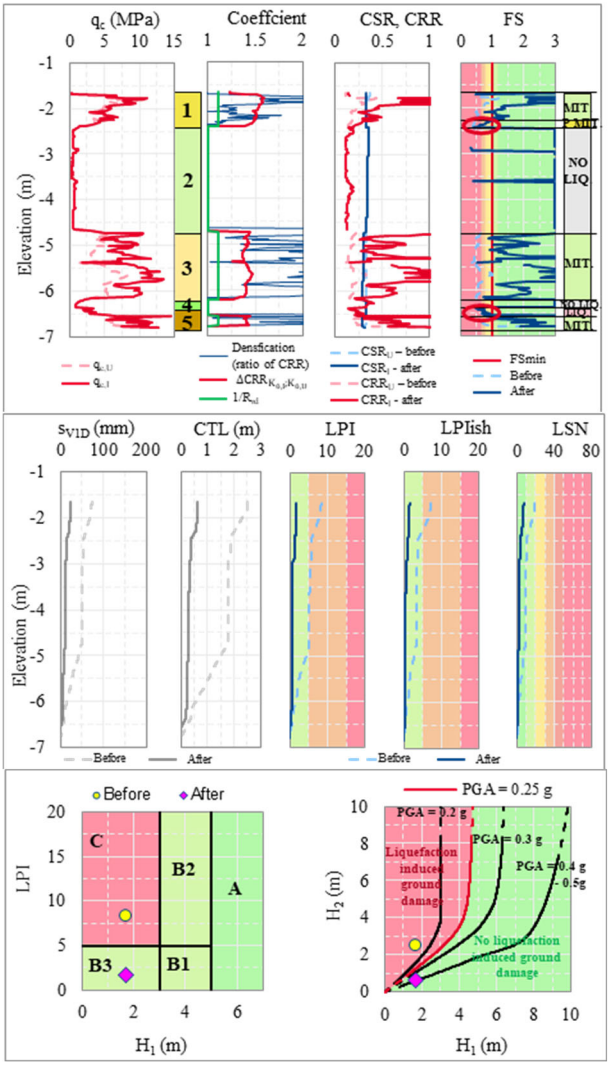

Summary	
S_{V1D} (mm)	23
H_1 (m)	1.7
CTL=H_2 (m)	0.6
LPI	2
LPIish	2
LSN	7
Ishirara (1985)	No damage
Towhata (2015)	B3

Figure 8. Liquefaction analysis after CMC reinforcement.

The final condition of the ground after CMC installation, considering the combined effects of densification, increase in K_0, and shear stress reduction, is reflected in the updated safety factor against liquefaction shown in Figure 8.

The analysis shows a significant improvement in liquefaction resistance across most of the soil profile. Two thin layers still exhibit safety factors below unity; however, these correspond to transitional zones between soil layers. Due to the limited thickness of these zones relative to the diameter of the CPT cone, the measured cone resistance may not accurately reflect the true soil strength. Even when conservatively including these transitional layers in the analysis, all liquefaction vulnerability indicators remain favorable. Based on this assessment, it can be concluded that the liquefaction risk has been effectively mitigated. While complete elimination of liquefaction is not strictly achieved, the installation of CMCs within the ground contributes to settlement control (23 mm) and overall structural stability.

6 CONCLUSION

CMCs offer a robust and versatile ground improvement solution for mitigating liquefaction risks in seismic-prone areas. Their effectiveness is driven by three key mechanisms: soil densification during installation, an increase in horizontal earth pressure, and a reduction in shear stress.

The methodology presented in this study demonstrates that CMCs enhance the seismic resilience of soils. A comprehensive design approach is essential for evaluating their performance, taking into account vulnerability indicators and post-liquefaction deformation, rather than focusing solely on safety factors against liquefaction.

Additionally, although not detailed in this paper, the seismic design of CMCs should also consider (i) the kinematic and inertial effects developing during the duration of the earthquake and (ii) their contribution on the post-seismic performance (deformation, geotechnical and structural verifications), regardless of whether liquefaction mitigation is complete or partial.

7 REFERENCES

Baez, J.I., and Martin, G.R. 1993. Advances in the art of liquefaction evaluation for level ground in the United States. *Proc. International Workshop on Earthquake Geotechnical Engineering*.

Baldi, G., Bellotti, R., Ghionna, V., Jamiolkowski, M., and Pasqualini, E. 1986. Interpretation of CPTs and CPTUs. *Proc. 2nd European Symposium on Penetration Testing*, Amsterdam.

Cristóvão, A., Nogueira, A., Hutchinson, R., Roberts, S., and Pinto, A. 2015. Installation effects of stone columns and their contribution to soil liquefaction mitigation. *Proc. 9th Portuguese Conference on Geotechnics*, Lisbon, Portugal.

Domingues, T.S., Borges, J.L., and Cardoso, A.S. 2009. Stone columns in embankments on soft soils: Analysis by the finite element method. *Geotechnical and Geological Engineering* 27(6), 667–679.

Green, R.A., Maurer, B.W., and Taylor, O.D.S. 2018. Influence of non-liquefied crust on the severity of surficial liquefaction manifestations. *Soil Dynamics and Earthquake Engineering* 104, 268–276.

Hashin, Z. 1983. Analysis of composite materials—A survey. *Journal of Applied Mechanics* 50(3), 481–505.

Idriss, I.M., and Boulanger, R.W. 2008. Soil liquefaction during earthquakes. *Earthquake Engineering Research Institute*, Oakland, CA.

Ishihara, K. 1985. Stability of natural deposits during earthquakes. *Proc. 11th International Conference on Soil Mechanics and Foundation Engineering*, San Francisco, 1, 321–376.

Ishihara, K., Yoshimine, M., and Towhata, I. 1977, 1985. Cyclic shear tests on saturated sand in torsional shear apparatus. *Soils and Foundations*.

Iwasaki, T., Tokida, K., and Tatsuoka, F. 1981. Soil liquefaction potential evaluation with use of the simplified procedure. *Proc. 1st International Conference on Recent Advances in Geotechnical Earthquake Engineering and Soil Dynamics*, St. Louis, Missouri, USA, April 28 – May 3, 1981.

Jacky, J. 1944. The coefficient of earth pressure at rest. *Journal of the Society of Hungarian Architects and Engineers* 78(22), 355–358.

Jamiolkowski, M. 2001. Soil behavior and soft ground construction. ASCE Geotechnical Special Publication No. 119.

Massarsch, K.R. 1991. Cone penetration testing for evaluation of soil compaction projects. *Proc. International Conference on Soil Mechanics and Foundation Engineering*, Stockholm.

Maurer, B.W., Green, R.A., and Taylor, O.D.S. 2015. Moving towards an improved index for assessing liquefaction hazard: Lessons from historical data. *Soils and Foundations* 55(4), 778–787.

Ménard, L. 1975. The Menard Pressuremeter: Interpretation and Application of Pressuremeter Test Results to Foundation Design. *Techniques Louis Ménard*, Paris, France, 45 pages

Priebe, H.J. 1995. The design of vibro replacement. *Ground Engineering* 28(10), 31–37.

Rayamajhi, D., Ashford, S.A., and Motamed, R. 2014. Shear stress reduction factor for rigid inclusions in liquefiable soils. *Soil Dynamics and Earthquake Engineering* 66, 290–296.

Robertson, P.K. 1986. In situ testing and its application to liquefaction and penetration resistance. *Transportation Research Record* 1022, 182–188.

Robertson, P.K., and Campanella, R.G. 1983. Interpretation of cone penetration tests: Part I—Sand. *Canadian Geotechnical Journal* 20(4), 718–733.

Salgado, R., Boulanger, R.W., and Mitchell, J.K. 1997. Lateral stress effects on CPT liquefaction resistance correlations. *Journal of Geotechnical and Geoenvironmental Engineering* 123(8), 726–735.

Siegel, T.C., NeSmith, W.M., NeSmith, W.M., and Cargill, P.E. 2007. Ground improvement resulting from installation of drilled displacement piles. Proc. *32nd Annual Conference on Deep Foundations (DFI)*, Colorado Springs, CO, USA, pp. 129–138.

Towhata, I., Yasuda, S., Yoshida, K., Motohashi, A., Sato, S., and Arai, M. 2016. Qualification of residential land from the viewpoint of liquefaction vulnerability. *Soils and Foundations* 56(4), 667–681.

van Ballegooy, S., Malan, P.J., Jacka, M.E., Lacrosse, V.I.M.F., Leeves, J.R., Lyth, J.E., and Cowan, H. 2012. Methods for characterising effects of liquefaction in terms of damage severity. Proc. *15th World Conference on Earthquake Engineering*, Lisbon, Portugal.

Youd, T.L., Idriss, I.M., Andrus, R.D., Arango, I., Castro, G., Christian, J.T., Dobry, R., Finn, W.D.L., Harder, L.F., Hynes, M.E., Ishihara, K., Koester, J.P., Liao, S.S.C., Marcuson, W.F., Martin, G.R., Mitchell, J.K., Moriwaki, Y., Power, M.S., Robertson, P.K., Seed, R.B., and Stokoe, K.H. II. 2001. Liquefaction resistance of soils: Summary report from the 1996 NCEER and 1998 NCEER/NSF workshops on evaluation of liquefaction resistance of soils. Journal of Geotechnical and Geoenvironmental Engineering 127(10), 817–833.

Zhang, G., Robertson, P.K., and Brachman, R.W.I. 2002. Estimating liquefaction-induced ground settlements from CPT for level ground. *Canadian Geotechnical Journal* 39(5), 1168–1180.